



ARTICLE

Chaoqun Chen¹, Jinrui Zhang¹, Yingqiu Zhang¹, Quentin Liu¹, Qingkai Yang¹, Yang Wang¹ · Yangfan Qi¹ · Han Li¹

Received: 5 September 2020 / Revised: 20 February 2021 / Accepted: 24 February 2021
© The Author(s) 2021. This article is published with open access

Abstract

Abstract text containing various symbols and numbers such as 42, 35, and 42.

Introduction

Introduction text containing various symbols and numbers such as 1-3 and 4-6.

Supplementary information
<https://doi.org/10.1038/s41418-021-00763-6>

- ✉ Correspondence
- ✉ Correspondence

Footnote text containing various symbols and numbers such as 7 and 3.

3000 ()

Immunofluorescence

20. 3% 15 0.2% 15 -100. 2% 30 1 (/ 63,). 5 8) 3. ().

Fluorescence recovery after photobleaching (FRAP)

2 42 42 42 120. 3 488 60%. 2.5 180 42 7).

Immunoblotting

(10 7.5, 150 1% -100, 0.1% 1% 3' 4 1 (). 5 95 4%

4 1 (4.0).

Lung cancer tissue specimens

Generation of stable cells

1, 2, 293 (1-) 1299 2 μ / 18= 1299 18= 293 / 2 21 1299 (2 μ /) 18=

CRISPR/Cas9-mediated gene ablation

9 42 1299 22 42 (// 42- #1, #2, 9()-2 (/ 458) 1299 48

96-

42

Protein purification and in vitro phase separation assay

42-(742-1316) ... 28 ... -21 ... (3) ... *Escherichia coli*. ... 0.4 ... 37 ... 12 ... 25 ... 7.5 ... 1 ... 42 ... (12.5 ... 7.5 ... 0.5 ... 400, 2000, 4000) ... 25% ... 600 ... 81, ...

mRNA sequencing and alternative splicing (AS) analysis

1299 ... 1299 ... 42 ... 9 ... 3p ... (18) ... 2000 ... 2.0.1.6 ...

Splicing assay via semi-quantitative RT-PCR

... (...) ... 37 ... (2p ...) ... (25 ...) ... 2% ...

Colony formation

6- ... (750 ...) ... 6- ... (2,000 ...) ... 37 ... 48 ... 2- ... 15 ... 0.1% ... 15 ...

Statistics

3.6.2 ... $P < 0.05$...

Results

Systematic survey reveals USP42 as a phase-separated DUB in the nucleus

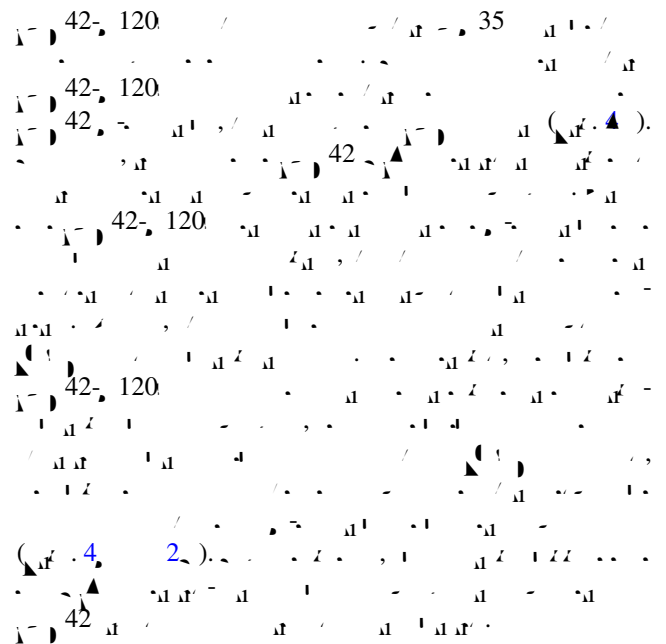
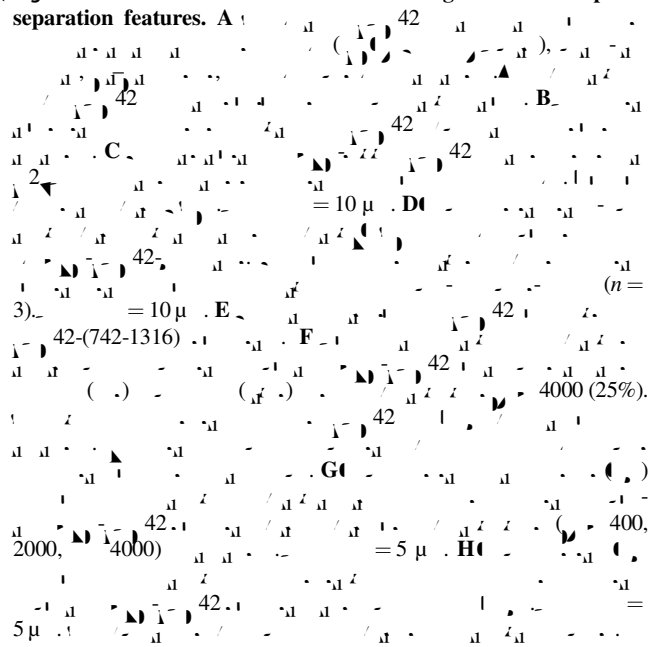
2, 3, 23 ... 71 ...

6
 8, 17, 24, 25
 1)
 36, 39, 42, 51, 7, 20,
 (1)
 36, 39,
 51
 6, 7, 20
 42
 1, 6-
 26, 27
 1, 6-
 39 42
 42
 42 2 -7
 42
 (3)
 2
 42
 42
 42
 42
 42
 (1)
 42

USP42 C-terminal disordered region confers phase separation features

42
 (28-30)
 42
 2 (2)
 31, 32
 ()
 33-35
 42

◀ Fig. 2 USP42 C-terminal disordered region confers phase separation features. A



USP42 controls PLRG1 phase separation and integration into nuclear speckles

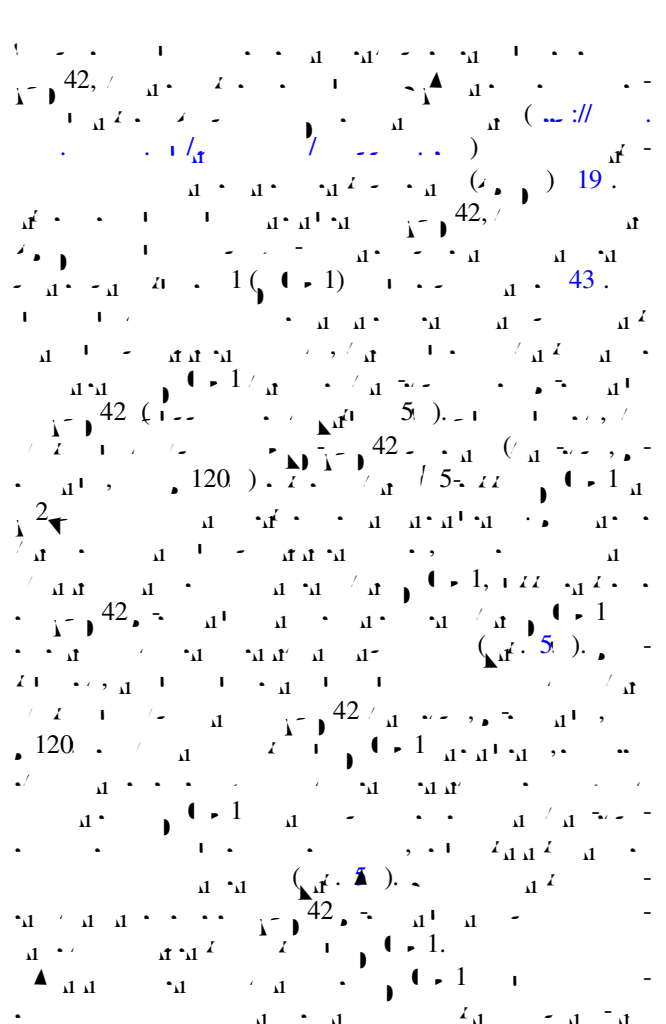
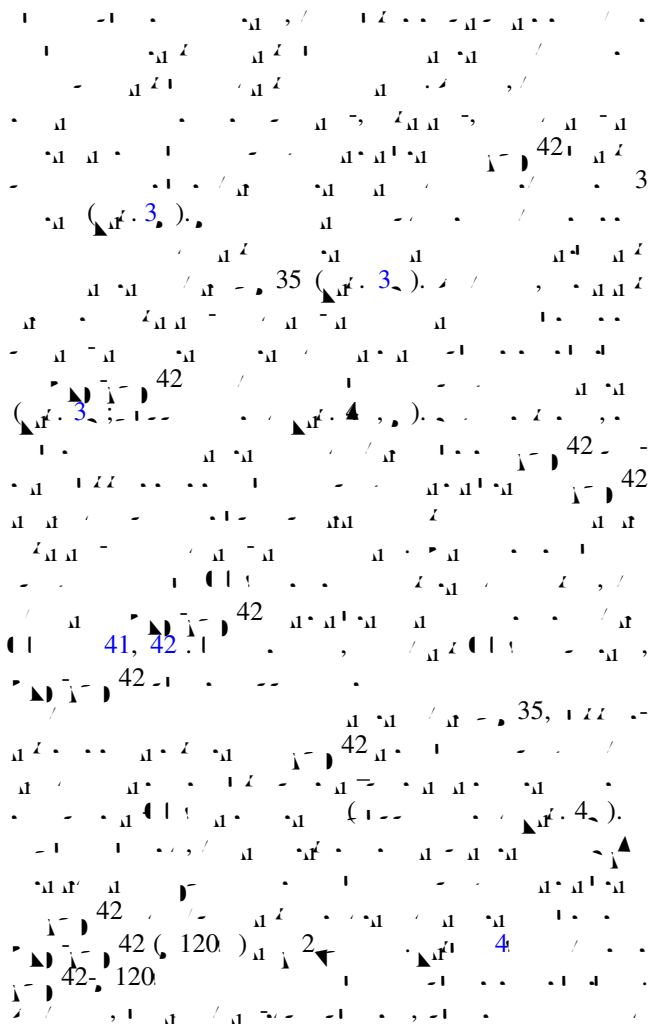




Fig. 3 Efficient nuclear speckle incorporation of USP42 relies on positively charged residues. **A** Confocal microscopy images of SC35 (green) and GFP-USP42 (red) in a nucleus. Scale bar = 10 μ m. **B** Confocal microscopy images of SC35 (green) and USP42 (red) in a nucleus. Scale bar = 10 μ m. **C** Schematic diagrams of various GFP-USP42 constructs: Δ P, Δ K, Δ R, Δ AR, Δ KR, and Δ RKR. **D** Confocal microscopy images and line graphs showing SC35 (green) and GFP-USP42 (red) intensity profiles for each construct. Scale bar = 10 μ m.

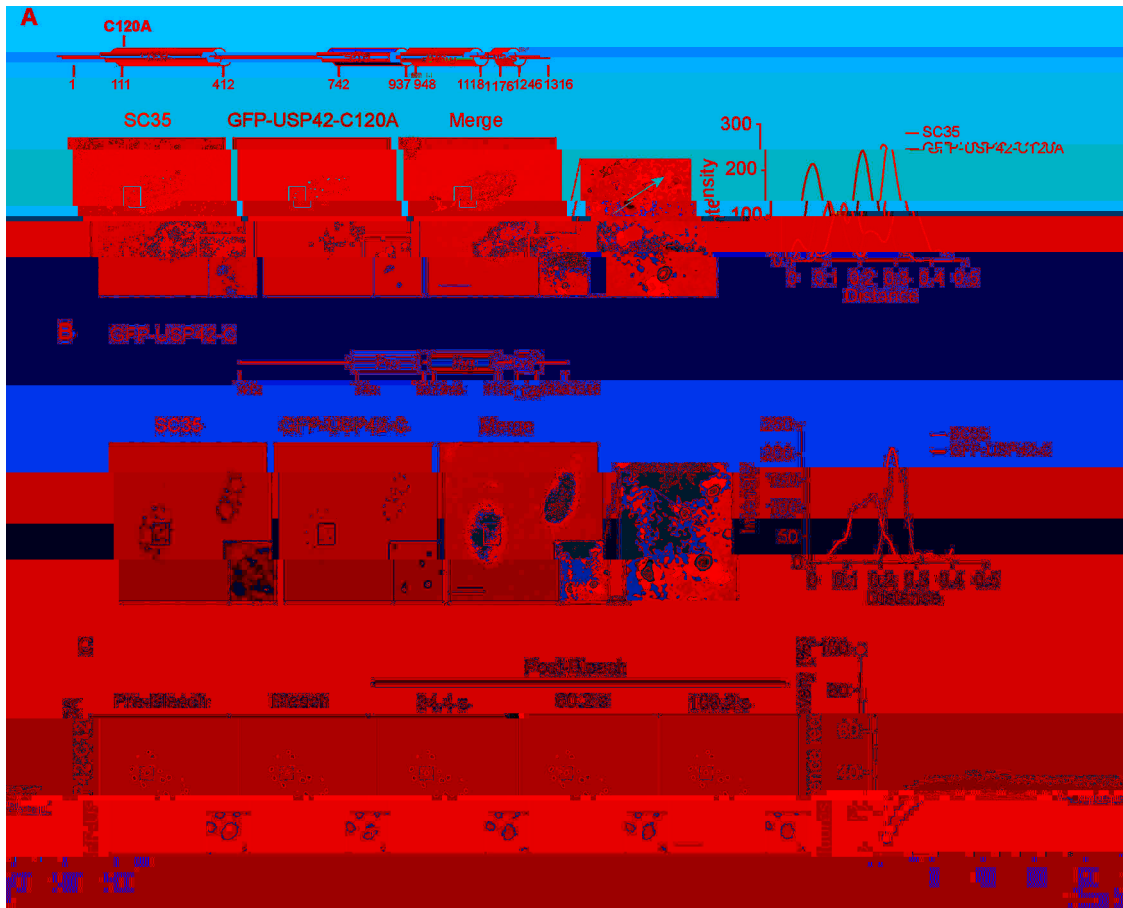


Fig. 4 USP42 DUB activity is required for its efficient nuclear speckle localization and phase separation. A, B

2. Δ 42-120 (n=3) = 10 μ m. C Δ 42-120 (n=3) = 10 μ m.

5. Δ 42-120 (n=3) = 10 μ m. 6. Δ 42-120 (n=3) = 10 μ m. 7. Δ 42-120 (n=3) = 10 μ m. 8. Δ 42-120 (n=3) = 10 μ m. 9. Δ 42-120 (n=3) = 10 μ m.

USP42 depletion hinders cell proliferation and alters nuclear speckle morphology

9. Δ 42-120 (n=3) = 10 μ m.

10. Δ 42-120 (n=3) = 10 μ m. 11. Δ 42-120 (n=3) = 10 μ m. 12. Δ 42-120 (n=3) = 10 μ m. 13. Δ 42-120 (n=3) = 10 μ m. 14. Δ 42-120 (n=3) = 10 μ m. 15. Δ 42-120 (n=3) = 10 μ m. 16. Δ 42-120 (n=3) = 10 μ m. 17. Δ 42-120 (n=3) = 10 μ m. 18. Δ 42-120 (n=3) = 10 μ m. 19. Δ 42-120 (n=3) = 10 μ m. 20. Δ 42-120 (n=3) = 10 μ m. 21. Δ 42-120 (n=3) = 10 μ m. 22. Δ 42-120 (n=3) = 10 μ m. 23. Δ 42-120 (n=3) = 10 μ m. 24. Δ 42-120 (n=3) = 10 μ m. 25. Δ 42-120 (n=3) = 10 μ m. 26. Δ 42-120 (n=3) = 10 μ m. 27. Δ 42-120 (n=3) = 10 μ m. 28. Δ 42-120 (n=3) = 10 μ m. 29. Δ 42-120 (n=3) = 10 μ m. 30. Δ 42-120 (n=3) = 10 μ m. 31. Δ 42-120 (n=3) = 10 μ m. 32. Δ 42-120 (n=3) = 10 μ m. 33. Δ 42-120 (n=3) = 10 μ m. 34. Δ 42-120 (n=3) = 10 μ m. 35. Δ 42-120 (n=3) = 10 μ m. 36. Δ 42-120 (n=3) = 10 μ m. 37. Δ 42-120 (n=3) = 10 μ m. 38. Δ 42-120 (n=3) = 10 μ m. 39. Δ 42-120 (n=3) = 10 μ m. 40. Δ 42-120 (n=3) = 10 μ m. 41. Δ 42-120 (n=3) = 10 μ m. 42. Δ 42-120 (n=3) = 10 μ m. 43. Δ 42-120 (n=3) = 10 μ m. 44. Δ 42-120 (n=3) = 10 μ m. 45. Δ 42-120 (n=3) = 10 μ m. 46. Δ 42-120 (n=3) = 10 μ m. 47. Δ 42-120 (n=3) = 10 μ m. 48. Δ 42-120 (n=3) = 10 μ m. 49. Δ 42-120 (n=3) = 10 μ m. 50. Δ 42-120 (n=3) = 10 μ m. 51. Δ 42-120 (n=3) = 10 μ m. 52. Δ 42-120 (n=3) = 10 μ m. 53. Δ 42-120 (n=3) = 10 μ m. 54. Δ 42-120 (n=3) = 10 μ m. 55. Δ 42-120 (n=3) = 10 μ m. 56. Δ 42-120 (n=3) = 10 μ m. 57. Δ 42-120 (n=3) = 10 μ m. 58. Δ 42-120 (n=3) = 10 μ m. 59. Δ 42-120 (n=3) = 10 μ m. 60. Δ 42-120 (n=3) = 10 μ m. 61. Δ 42-120 (n=3) = 10 μ m. 62. Δ 42-120 (n=3) = 10 μ m. 63. Δ 42-120 (n=3) = 10 μ m. 64. Δ 42-120 (n=3) = 10 μ m. 65. Δ 42-120 (n=3) = 10 μ m. 66. Δ 42-120 (n=3) = 10 μ m. 67. Δ 42-120 (n=3) = 10 μ m. 68. Δ 42-120 (n=3) = 10 μ m. 69. Δ 42-120 (n=3) = 10 μ m. 70. Δ 42-120 (n=3) = 10 μ m. 71. Δ 42-120 (n=3) = 10 μ m. 72. Δ 42-120 (n=3) = 10 μ m. 73. Δ 42-120 (n=3) = 10 μ m. 74. Δ 42-120 (n=3) = 10 μ m. 75. Δ 42-120 (n=3) = 10 μ m. 76. Δ 42-120 (n=3) = 10 μ m. 77. Δ 42-120 (n=3) = 10 μ m. 78. Δ 42-120 (n=3) = 10 μ m. 79. Δ 42-120 (n=3) = 10 μ m. 80. Δ 42-120 (n=3) = 10 μ m. 81. Δ 42-120 (n=3) = 10 μ m. 82. Δ 42-120 (n=3) = 10 μ m. 83. Δ 42-120 (n=3) = 10 μ m. 84. Δ 42-120 (n=3) = 10 μ m. 85. Δ 42-120 (n=3) = 10 μ m. 86. Δ 42-120 (n=3) = 10 μ m. 87. Δ 42-120 (n=3) = 10 μ m. 88. Δ 42-120 (n=3) = 10 μ m. 89. Δ 42-120 (n=3) = 10 μ m. 90. Δ 42-120 (n=3) = 10 μ m. 91. Δ 42-120 (n=3) = 10 μ m. 92. Δ 42-120 (n=3) = 10 μ m. 93. Δ 42-120 (n=3) = 10 μ m. 94. Δ 42-120 (n=3) = 10 μ m. 95. Δ 42-120 (n=3) = 10 μ m. 96. Δ 42-120 (n=3) = 10 μ m. 97. Δ 42-120 (n=3) = 10 μ m. 98. Δ 42-120 (n=3) = 10 μ m. 99. Δ 42-120 (n=3) = 10 μ m. 100. Δ 42-120 (n=3) = 10 μ m.



Fig. 5 USP42 associates with and drives the phase separation of PLRG1. **A**, 2 × 42 (120) = 10 μ. **B**, 2 × 42 (120) = 10 μ. **C**, 42 (150) = 5 μ. **D**, 42 (150) = 5 μ.



Fig. 5 Identification of USP42 and PLRG1 as interactors of Cas9. **A**, Western blot analysis of USP42 and PLRG1 levels in H1299 cells treated with Cas9. The blots were probed with anti-USP42 and anti-PLRG1 antibodies. Tubulin was used as a loading control. The p-values for the USP42 and PLRG1 blots are $P=0.0132$ and $P=0.0002$, respectively. **B**, Co-immunoprecipitation (Co-IP) assays. H1299 cells were treated with Cas9 and immunoprecipitated with anti-USP42 or anti-PLRG1 antibodies. The immunoprecipitates were probed with anti-Cas9, anti-USP42, or anti-PLRG1 antibodies. The blots show the presence of Cas9, USP42, and PLRG1 in the immunoprecipitates. **C**, 2D gel electrophoresis image of the USP42-precipitated fraction. The spots are labeled with their pI and pK values. The spots are color-coded: red for spots that are significantly enriched in the USP42-precipitated fraction compared to the control. **D**, 2D gel electrophoresis image of the PLRG1-precipitated fraction. The spots are labeled with their pI and pK values. The spots are color-coded: red for spots that are significantly enriched in the PLRG1-precipitated fraction compared to the control.



... 41, 53-55 ... 42 /
... 56 ... 42 /
... 42 ...

22. [2013;8:2281–308.](#)
23. [2019;37:1435–45.](#)
24. [2013;93:1289–315.](#)
25. [2014;1843:114–28.](#)
26. [2017. \[:// dx.doi.org/10.19185/201702000010.\]\(#\)](#)
27. [2019;176:419–34.](#)
28. [2020;48: 354– 359. \[:// dx.doi.org/10.1093/ije/dyaa0847.\]\(#\)](#)
29. [2014;30:2501–2.](#)
30. [2018;7: 31486. \[:// dx.doi.org/10.7554/2018.31486.\]\(#\)](#)
31. [2018;46: 329– 37.](#)
32. [2012;28:503–9.](#)
33. [2017;292:19110–20.](#)
34. [2017;9:1118–25.](#)
35. [2017;44:18–30.](#)
36. [2015;34:23–30.](#)
37. [1991;10:3467–81.](#)
38. [2017;45:10350–68.](#)
39. [1990;343:437–41.](#)
40. [2017;130:4180–92.](#)
41. [2006;288:664–75.](#)
42. [2011;3: 000646. \[:// dx.doi.org/10.1101/000646.\]\(#\)](#)
43. [2004;15:3876–90.](#)
44. [2011;30:4921–30.](#)
45. [1998;20:46–50.](#)
46. [2000;19:6569–81.](#)
47. [2005;280:42863–76.](#)
48. [2018;293:3892–903.](#)
49. [2017;357: 4382. \[:// dx.doi.org/10.1126/science.1254382.\]\(#\)](#)
50. [2018;174:688–99 16.](#)
51. [2019;76:295–305.](#)
52. [2019. \[:// dx.doi.org/10.1038/41573-019-00069-9.\]\(#\)](#)
53. [2003;162:981–90.](#)
54. [2008;182:1083–97.](#)
55. [2020;219: 201904046. \[:// dx.doi.org/10.1083/201904046.\]\(#\)](#)
56. [2014;289:34862–70.](#)
57. [2010;38:137–43.](#)
58. [2015;147:32–54.](#)